

# Simultaneous determination of ribonucleoside and deoxyribonucleoside triphosphates in biological samples by hydrophilic interaction liquid chromatography coupled with tandem mass spectrometry

Ziqing Kong<sup>1,†</sup>, Shaodong Jia<sup>1,†</sup>, Anna Lena Chabes<sup>1</sup>, Patrik Appelblad<sup>2,3</sup>, Richard Lundmark<sup>4,5</sup>, Thomas Moritz<sup>6</sup> and Andrei Chabes<sup>1,5,\*</sup>

<sup>1</sup>Department of Medical Biochemistry and Biophysics, Umeå University, SE-901 87 Umeå, Sweden, <sup>2</sup>Department of Pharmacology and Clinical Neuroscience, Umeå University, SE-901 87, Umeå, Sweden, <sup>3</sup>Merck Chemicals and Life Science AB, SE 169-03 Solna, Sweden, <sup>4</sup>Dept. of Integrative Medical Biology, Umeå University, SE-901 87 Umeå, Sweden, <sup>5</sup>Laboratory for Molecular Infection Medicine Sweden (MIMS), Umeå University, SE-901 87 Umeå, Sweden and <sup>6</sup>Umeå Plant Science Centre (UPSC), Dept. of Forest Genetics and Plant Physiology, SLU, SE-901 87 Umeå, Sweden

Received February 01, 2018; Revised February 27, 2018; Editorial Decision March 07, 2018; Accepted March 08, 2018

## ABSTRACT

Information about the intracellular concentration of dNTPs and NTPs is important for studies of the mechanisms of DNA replication and repair, but the low concentration of dNTPs and their chemical similarity to NTPs present a challenge for their measurement. Here, we describe a new rapid and sensitive method utilizing hydrophilic interaction liquid chromatography coupled with tandem mass spectrometry for the simultaneous determination of dNTPs and NTPs in biological samples. The developed method showed linearity ( $R^2 > 0.99$ ) in wide concentration ranges and could accurately quantify dNTPs and NTPs at low pmol levels. The intra-day and inter-day precision were below 13%, and the relative recovery was between 92% and 108%. In comparison with other chromatographic methods, the current method has shorter analysis times and simpler sample pre-treatment steps, and it utilizes an ion-pair-free mobile phase that enhances mass-spectrometric detection. Using this method, we determined dNTP and NTP concentrations in actively dividing and quiescent mouse fibroblasts.

## INTRODUCTION

The balance and the overall concentration of the four dNTPs are tightly regulated by multiple mechanisms (1). Defects in dNTP metabolism lead to increased mutation rates (2–5) and are associated with various human disorders (6,7). The overall concentration of dNTPs is very low in non-dividing cells, where dNTPs are used primarily for DNA repair or mitochondrial DNA (mtDNA) synthesis, but it increases in dividing cells in S phase, when dNTPs are used for the replication of nuclear DNA (8). However, even in actively dividing budding yeast cells, the concentration of dNTPs is still between ~40- and ~200-fold lower than the concentration of the corresponding NTPs, depending on the individual dNTP/NTP pair (9). This difference in the concentrations of dNTPs and NTPs presents a challenge for DNA polymerases, which incorporate significant amounts of NTPs into DNA (10,11). The amount of ribonucleotides incorporated into DNA directly depends on the individual dNTP/NTP ratios (10). Therefore, information about the cellular concentration of the four canonical dNTPs (dCTP, dTTP, dATP and dGTP) and four canonical NTPs (CTP, UTP, ATP and GTP) both in dividing and in quiescent cells is important for the analysis of the biochemical properties of DNA polymerases and the studies of incorporation and repair of ribonucleotides in DNA.

Several analytical methods have been established to quantify cellular dNTPs and NTPs. Nevertheless, the identification and the quantification of cellular dNTPs and NTPs remain challenging, and surprisingly little is known

\*To whom correspondence should be addressed. Tel: +46736205446; Email: andrei.chabes@medchem.umu.se

†The authors wish it to be known that, in their opinion, the first two authors should be regarded as Joint First Authors.

about dNTP and NTP concentrations in various organisms and tissues. Although enzymatic DNA polymerase assays used for measurements of dNTPs are sensitive (12–14), the presence of cellular metabolites, including NTPs, can inhibit DNA polymerases and influence the results. Furthermore, this approach cannot be used for the simultaneous quantification of NTPs. The current HPLC-based approaches have other limitations. The reverse phase chromatography methods with conventional mobile phases for separation of ribo- and deoxyribonucleotides (15–17) have poor separation of dNTPs and NTPs due to their high hydrophilicity. Strong anion exchange methods (18,19) are not compatible with mass spectrometry (MS) because these methods require high concentrations of non-volatile salts in the mobile phase. Other concerns are interference from baseline noise and low sensitivity, which require the use of a large sample size and large injection volumes. Furthermore, the sample extraction and the chromatographic separation in these methods are time-consuming. Although HPLC–MS/MS methods have been used for the specific measurement of intracellular dNTPs with high sensitivity, these methods used ion-pair interactions (20,21). However, ion-pair reagents in the mobile phase (e.g. heptafluorobutyric acid or phosphoric acid) are rarely volatile acids and can affect the performance of MS in ionization suppression of the analytes and can contaminate the ion source as well as the HPLC systems.

Polar compounds can be efficiently separated by hydrophilic interaction liquid chromatography (HILIC) where a polar stationary phase is used together with a mixture of water or aqueous buffer solutions and organic solvents (mainly acetonitrile or low molecular alcohols such as MeOH) as the mobile phase. The HILIC separation mode allows polar compounds to be successfully retained on the stationary phase and eluted by increasing the aqueous portion in the mobile phase. Depending on the stationary phase properties, it is also possible to utilize underlying electrostatic interactions of either weak or strong character. (22–25). Many volatile buffers or acid/base modifiers can therefore be used as mobile phase additives to improve the chromatographic behavior of the analytes, especially for ionizable compounds. Another advantage of HILIC is the compatibility of its mobile phase with electrospray ionization. Johnsen *et al.* reported a method using two polymer sulfobetaine-based ZIC-pHILIC columns in tandem for the simultaneous separation of eight dNTPs and NTPs in *Escherichia coli* cell samples with an analysis time of ~70 min (26). However, because the detection was UV-based, the sensitivity and specificity of the method were not sufficient for the analysis of samples with low dNTP concentrations, e.g. quiescent mammalian cells. Another recently developed ion-pairing-free HPLC–MS/MS method detects the four dNTPs and ATP, but not the other three NTPs (27).

In the current study, we developed and validated a fast, sensitive, and simple ion-pairing-free method for the determination of the eight canonical dNTPs and NTPs using a silica phosphorylcholine-based ZIC-cHILIC column coupled with tandem mass spectrometry, and we used this method to determine the concentrations of dNTPs and

NTPs in actively dividing and in quiescent mouse Balb/3T3 fibroblasts.

## MATERIALS AND METHODS

### Chemicals

dNTP and NTP standards, including 2'-deoxyadenosine 5'-triphosphate (dATP); 2'-deoxythymidine 5'-triphosphate (dTTP); 2'-deoxyguanosine 5'-triphosphate (dGTP); 2'-deoxycytidine 5'-triphosphate (dCTP); adenosine 5'-triphosphate (ATP); uridine 5'-triphosphate (UTP); guanosine 5'-triphosphate (GTP); and cytidine 5'-triphosphate (CTP) were from Thermo Fisher Scientific. Stable isotope-labeled internal standards, including adenosine-<sup>13</sup>C<sub>10</sub>, <sup>15</sup>N<sub>5</sub> 5'-triphosphate (ATP<sup>13</sup>C<sub>10</sub>, <sup>15</sup>N<sub>5</sub>); uridine-<sup>13</sup>C<sub>9</sub>, <sup>15</sup>N<sub>2</sub> 5'-triphosphate (UTP<sup>13</sup>C<sub>9</sub>, <sup>15</sup>N<sub>2</sub>); guanosine-<sup>13</sup>C<sub>10</sub> 5'-triphosphate (GTP<sup>13</sup>C<sub>10</sub>); cytidine-<sup>15</sup>N<sub>3</sub> 5'-triphosphate (CTP<sup>15</sup>N<sub>3</sub>); 2'-deoxyadenosine <sup>13</sup>C<sub>10</sub>, <sup>15</sup>N<sub>5</sub> 5'-triphosphate (dATP<sup>13</sup>C<sub>10</sub>, <sup>15</sup>N<sub>5</sub>); 2'-deoxyguanosine <sup>13</sup>C<sub>10</sub>, <sup>15</sup>N<sub>5</sub> 5'-triphosphate (dGTP<sup>13</sup>C<sub>10</sub>, <sup>15</sup>N<sub>5</sub>); 2'-deoxythymidine <sup>13</sup>C<sub>10</sub>, <sup>15</sup>N<sub>2</sub> 5'-triphosphate (dTTP<sup>13</sup>C<sub>10</sub>, <sup>15</sup>N<sub>2</sub>); and 2'-deoxycytidine <sup>13</sup>C<sub>9</sub>, <sup>15</sup>N<sub>3</sub> 5'-triphosphate (dCTP<sup>13</sup>C<sub>9</sub>, <sup>15</sup>N<sub>3</sub>), were from Sigma-Aldrich (part of Merck Life Science, Darmstadt Germany). Trichloroacetic acid (TCA) and magnesium chloride (MgCl<sub>2</sub>) were from Scharlau (Scharlab S.L., Spain), and HPLC-grade acetonitrile and methanol were from Thermo Fisher Scientific. Deionized water was produced with the Milli-Q Q-POD system (Merck Life Science, Darmstadt Germany). Freon (1,1,2-trichloro-1,2,2-trifluoroethane), trioctylamine, LC–MS–grade ammonium hydroxide solution (25%), LC–MS–grade acetic acid, LC–MS–grade ammonium acetate, phosphate-buffered saline (PBS), horse serum, and Dulbecco's Modified Eagle's Medium (DMEM) were all from Sigma-Aldrich (part of Merck Life Science, Darmstadt Germany). Penicillin/streptomycin, L-glutamine, and trypsin/EDTA were from Gibco Life Technologies. The Oasis WAX solid phase extraction (SPE) cartridge, 30 mg, 60 μm was from Waters, and the chromatographic column ZIC-cHILIC, 3 μm, 150 × 2.1 mm PEEK was from Merck Life Science, Darmstadt Germany.

### Standard solutions

Stock solutions of each standard were prepared at a concentration of 10 mM in water and stored at –20°C until use. The working solutions were prepared by diluting stock solutions to 100 nM, and 600 μl were loaded onto the Oasis WAX SPE cartridge. The different solutions for calibration curves were made fresh by serial dilution of stock solutions with water. The isotope-labeled internal standard solution was freshly mixed and diluted with water to a concentration of 10 mM for dNTPs and 100 mM for NTPs.

### Chromatographic and mass-spectrometric analysis

Intracellular concentrations of dNTPs and NTPs were analyzed on an LC–MS/MS system composed of an Agilent 1290 UHPLC (Agilent Technologies, Waldbron, Germany) coupled with an Agilent 6490 triple quadrupole mass spectrometer (Agilent Technologies, Santa Clara, CA, USA).

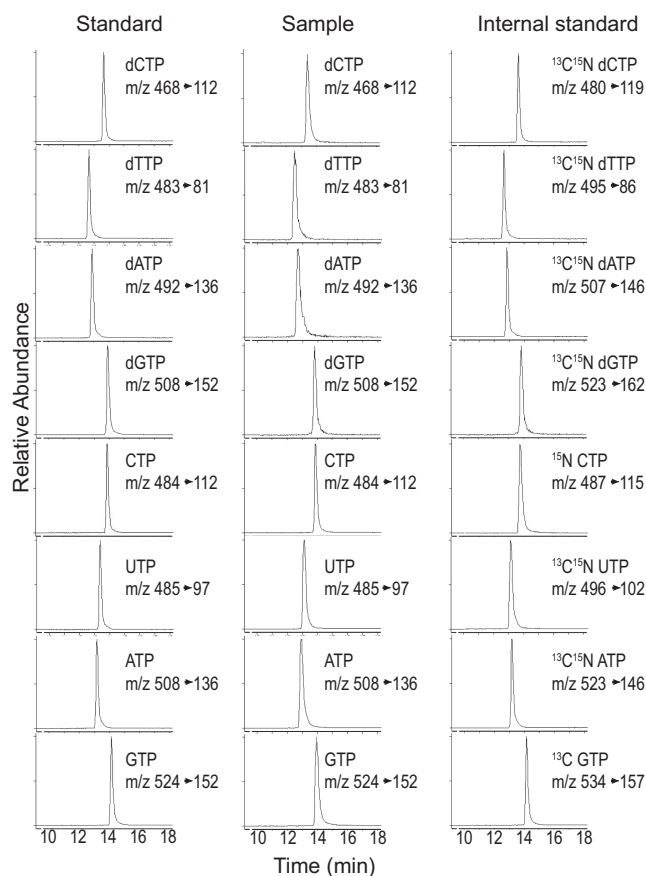


**Figure 1.** ZIC-chILIC-HPLC multiple reaction monitoring (MRM) chromatograms of all dNTP and NTP analytes in a standard mixture solution and in extracts from Balb/3T3 fibroblasts and their <sup>13</sup>C<sup>15</sup>N-labeled internal standards. The MRM transitions are shown for each of the target analytes.

The analytes were separated on a 150 × 2.1 mm ZIC-chILIC column with 3 μm particles. A stepwise gradient program was applied with mobile phase A (10 mM ammonium acetate, adjusted to pH 7.7 with aqueous ammonia solution, in 90/10 water/acetonitrile) and mobile phase B (2.5 mM ammonium acetate adjusted to pH 7.7 with aqueous ammonia solution in 90/10 acetonitrile/water) delivered at a flow rate of 200 μl min<sup>-1</sup> (Table 1). The HPLC eluate was introduced into the mass spectrometer through an electroionization spray interface in which analytes and internal standards were ionized and carried a positive charge. The injection volume was 5 μl, and the separation was carried out at 35°C. The LC-MS/MS instrument was operated in multiple-reaction-monitoring (MRM) mode. MRM transitions (precursor ions and product ions) are listed in Figure 1 and Supplementary Table S1, which also lists the collision energies. The in-source parameters were set as follows: gas temperature 200°C; gas flow 14 l·min<sup>-1</sup>; nebulizer pressure 20 psi; sheath gas temperature 320°C; nebulizer gas flow 10 l·min<sup>-1</sup>; capillary voltage 4000 V; and nozzle voltage 400 V. Each HILIC-MS/MS run was divided into three sections, in which the eluent from the column was diverted to waste from 0 to 7 min and from 19 to 23 min in order to minimize the contamination of the ion source.

## Cell culture

Mouse Balb/3T3 fibroblasts (ATCC CCL-163) were maintained in DMEM supplemented with 10% horse serum. For unsynchronized samples, cells were seeded and collected the following day. For serum-deprived samples, cells were seeded in DMEM with 10% horse serum. On the following day, cells were washed twice with PBS and then cultured in DMEM with 0.6% horse serum for 24 or 48 h.

For analysis of dNTP and NTP pools in logarithmically growing cells, 6 × 10<sup>5</sup> cells were seeded onto 10 cm plates in triplicate. For the quiescent, serum-deprived cells, 4 × 10<sup>5</sup> cells were seeded onto 10 cm plates in triplicate. For cell cycle analysis by flow cytometry, cells were seeded on one 10 cm plate in the same way and in parallel with the cells seeded for nucleotide pool measurements. The cells were trypsinized, counted, and collected by centrifugation. The nuclei were extracted and stained using the CyStain DNA 2 step kit (Sysmex Partec GmbH) and analyzed on a CCA-I flow cytometer (Sysmex Partec GmbH).

## Preparation of dNTP and NTP extracts

Cells were washed twice with ice-cold sodium chloride (9 g/l) and harvested using a cell scraper in 550 μl of ice-cold 15% TCA supplemented with 30 mM magnesium chloride. The resulting solution was pulse-vortexed (Intellimixer) at 99 rpm for 10 min at 4°C and centrifuged at 20 000 × g for 1 min at 4°C, and the supernatant was extracted twice with 1.4× the volume of Freon (78% v/v)-trioctylamine (22%, v/v). After Freon extraction, 5 μl 0.5% acetic acid and 5 μl isotope-labeled internal standards were added, and the mixture was loaded onto an Oasis weak anion exchange (WAX) SPE cartridge. Interfering compounds were eluted off the cartridges in two steps with 1 ml ammonium acetate buffer (pH was adjusted to 4.5 with acetic acid) and 1 ml 0.5% ammonia aqueous solution in methanol (v/v), and the analytes were eluted from the cartridge with 2 mL methanol/water/ammonia solution (80/15/5, v/v/v) into a glass tube and then evaporated to dryness using a centrifugal evaporator at a temperature below 37°C. The residue was reconstituted in 50 μl sample injection solution (acetonitrile/water/100 mM ammonium acetate, 30/9/1, v/v/v) for the HILIC-MS/MS analysis.

## Quantitative method

Calibration curve samples and quality control (QC) samples for all dNTPs and NTPs were prepared in aqueous matrix (28). The concentration of intracellular compounds was calculated using calibration curves and was expressed as pmol/10<sup>6</sup> cells. A calibration curve for each dNTP and NTP was obtained by quadratic regression analysis with 1/X<sup>2</sup> weighting based on the peak area ratio of the analyte to the internal standard. Calibration curves with a coefficient of determination (*R*<sup>2</sup>) higher than 0.99 were acceptable. The quantitative analysis of intracellular dNTPs and NTPs in Balb/3T3 cell extracts was based on the peak area ratio of the analytes to the internal standard.

**Table 1.** HPLC gradient for the separation of dNTPs and NTPs on the ZIC-cHILIC column

Time (min)	Mobile phase A (%)	Mobile phase B (%)	Flow rate ( $\mu\text{l min}^{-1}$ )
0.0	20	80	200
7.0	20	80	200
12.0	40	60	200
17.0	40	60	200
19.0	20	80	200
23.0	20	80	200

### Method validation design

The developed method was validated in terms of linearity, precision, lower limit of quantification (LLOQ), relative recovery, and stability. Considering the different levels of dNTPs and NTPs in biological samples, the calibration curves were constructed in two different ranges against five calibration levels by plotting the peak area ratios of analytes to each of their corresponding isotope-labeled internal standards. The intra-day precision was assessed with QC samples containing isotope-labeled dNTP and NTP internal standards at three concentration levels by injecting three times during the day, while the inter-day precision was assessed by injecting samples for three consecutive days. The relative recovery was tested by the spiking experiments with the QC sample at a medium level into the Balb/3T3 sample as follows: 450  $\mu\text{l}$  cell extracts were spiked with 50  $\mu\text{l}$  pure water (blank sample) or 50  $\mu\text{l}$  standard mixture at medium QC level (spiked sample), and 450  $\mu\text{l}$  pure water was added with 50  $\mu\text{l}$  standard mixture to calculate the amount spiked. The resulting solutions were loaded onto the WAX SPE cartridges after adding isotope-labeled internal standards and acetic acid. The relative recovery was calculated as  $[(\text{amount found in the spiked sample} - \text{amount found in the sample})/\text{amount added}] \times 100$ . The LLOQ was chosen as the concentration of the lowest calibration standard. The analysis of dNTP and NTP stability during storage was performed independently at  $-20^\circ\text{C}$  in Balb/3T3 cell samples spiked with standards at medium QC level. Spiked Balb/3T3 samples were analyzed fresh and after 24, 48 and 72 h of storage.

### Microscopic analysis of cell size

Cells were seeded onto 12 mm poly-D-lysine-coated coverslips (Neuvitro Corporation). After 24 h in 10% horse serum DMEM, cells were rinsed with PBS and either fixed in 3% paraformaldehyde for 20 min or grown for an additional 48 h in 0.6% horse serum DMEM followed by paraformaldehyde fixation. Paraformaldehyde-fixed coverslips were washed with PBS, blocked in 5% goat serum/0.05% saponin in PBS, and incubated with primary anti-CD44 antibody (Abcam) at 1:400 dilution in 1% goat serum/0.05% saponin in PBS for 1 h at room temperature. After washing three times for 5 min in 1% goat serum/0.05% saponin in PBS, coverslips were incubated with secondary Alexa Fluor 568-conjugated antibody at 1:300 dilution and DAPI at 1:50 000 dilution for 1 h. Confocal Z-stacks were obtained from 12 representative cells using a Zeiss Cell Observer Spinning Disk Confocal controlled by the ZEN interface with an Axio Observer.Z1 inverted microscope with a  $63 \times$  lens (Plan-Apochromat 1.40 Oil DIC M27) equipped

with an iXon Ultra EMCCD camera from ANDOR. Segmentation of the CD44 and DAPI signals and subsequent cell volume analysis was performed using the surface analysis tool Imaris V7.5 (Bitplane).

## RESULTS

### Sample preparation

To wash the cells and to quench cellular metabolism, we used ice-cold saline (0.9% [w/v] NaCl) (29). TCA was used to lyse the cells and to extract dNTPs and NTPs (30). Methods using two-step SPE procedures with reverse phase (RP) C18 SPE and WAX SPE have been reported for the pre-treatment of biological samples before dNTP and NTP analysis (26) The RP C18 SPE step was intended to remove the less polar compounds, while the WAX SPE step was for retaining the negatively charged compounds. To simplify the experimental procedure, we only used the WAX SPE step, but used 0.5% aqueous ammonia solution in methanol (v/v) instead of pure methanol for washing off the interferences because the interaction between the triphosphate group and the WAX functional group was strong enough.

### Separation and detection of dNTPs and NTPs by cHILIC-MS/MS

The first step in our evaluation was to identify and develop an effective HPLC separation. A silica phosphorylcholine-based ZIC-cHILIC stationary phase provided the best results in terms of selectivity. The initial efforts involved the optimization of mobile phases (in terms of organic content and salt concentration), loading buffers, flow rate, and gradient profile. The choice of the optimal mobile phases was related not only to electrospray ionization and MS compatibility, but also to separation efficiency and chromatographic resolution. All compounds were detected with good peak shapes, the separations among the eight dNTPs and NTPs were sufficient, and no isotopic interference was observed (Figure 1 and Supplementary Figure S1).

### Method validation

Based on the results of the analysis of standard solutions of dNTPs and NTPs at five concentration levels, the method was shown to exhibit good linearity in the concentration range with coefficients of determination ( $R^2$ ) greater than 0.99 for all dNTPs and NTPs (Table 2). The intra- and inter-day precision values, expressed as CV%, are summarized in Table 3. The within-day coefficients of variation (CVs,  $n = 3$ ) were  $<12.7\%$  and  $8.1\%$  for dNTPs and NTPs, respectively, and the inter-day precision was  $<10.5\%$  and

12.7% for dNTPs and NTPs, respectively. The stability of dNTPs and NTPs in extracts from Balb/3T3 cells at  $-20^{\circ}\text{C}$  was tested for a 72 h period, and no significant differences were found among mean values of dNTPs and NTPs using Student's t-test. Thus, dNTPs and NTPs in extracts from Balb/3T3 cells are stable at  $-20^{\circ}\text{C}$  for at least 72 h.

### Measurement of dNTP and NTP concentrations in Balb/3T3 mouse fibroblasts

The levels of dNTPs in eukaryotic cells vary according to the cell cycle, whereas the levels of NTPs are relatively constant (1,5). The dNTP levels are high in S phase—when DNA synthesis occurs—and low in  $G_1$  phase and in quiescent cells (8). To test the sensitivity of the developed LC-MS/MS method on biological samples, we measured dNTP and NTP amounts in logarithmically growing cell cultures with a mixed population of cells in all different phases of the cell cycle and in serum-starved quiescent cells that are predominantly in  $G_1/G_0$ . The cell cycle profiles were verified using flow cytometry analysis (Figure 2A). The cells were counted and the amount of dNTPs and NTPs were determined (Figure 2B and C and Table 4). The dNTP pools in quiescent cells were on average only 14% of those in the actively dividing cells, whereas the NTP pools in the serum-starved cells were on average 70% of the actively dividing cells. Because the NTP pools are less affected by the cell cycle phase, the ratios between the NTPs and the corresponding dNTPs increased between 2.5- to 10-fold in quiescent cells compared to logarithmically growing cells (Table 5). To calculate the actual concentration of dNTPs and NTPs in the cells, we measured the average cell volume in a mixed population of logarithmically growing cells as well as in quiescent cells using confocal microscopy. The outer membrane of the cells was visualized using fluorescently labeled antibodies, and the nuclei were labeled with DAPI. The average cell volumes were  $3026\ \mu\text{m}^3$  for the logarithmically growing cells and  $3212\ \mu\text{m}^3$  for the quiescent cells (Figure 2D). Using the average cell volumes, we calculated the dNTP and NTP concentrations in the cells (Table 6).

### DISCUSSION

The fidelity and processivity of DNA polymerases are affected both by the overall dNTP concentration and by the balance among the individual dNTPs that are present *in vivo* or in the test tube (3,4,31–38). Furthermore, these processes are also affected by the presence of NTPs (9,10). Therefore, knowledge about the intracellular concentrations of both dNTPs and NTPs is required both for *in vivo* and *in vitro* studies of DNA replication.

Here, we report a method for direct and simultaneous determination of all eight canonical dNTPs and NTPs. We show that this method is sensitive enough for quantification of dNTPs in quiescent Balb/3T3 fibroblasts that are known to have very low dNTP levels. The sensitivity of this method is expected to be high enough to measure dNTP concentrations in other types of non-dividing cells such as neurons, biopsies of differentiated tissues, and even mitochondria (provided that nucleotide concentrations do not change during isolation of mitochondria). Fur-

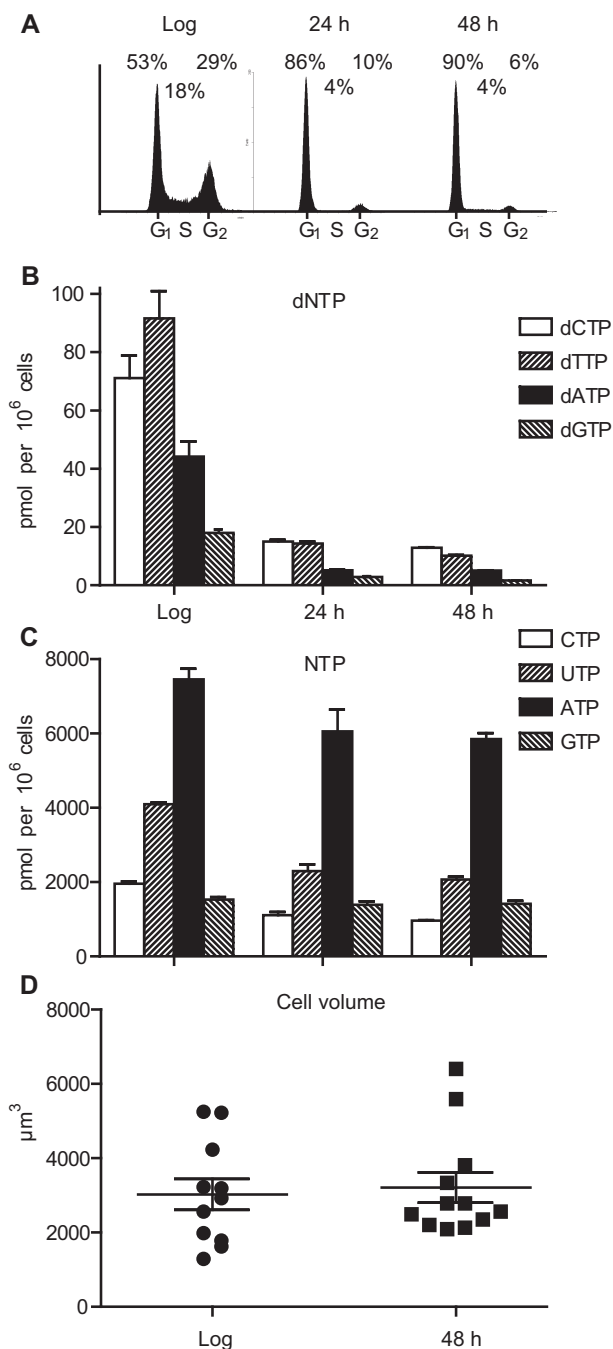


**Figure 2.** Determination of the dNTP and NTP concentrations in actively dividing and quiescent mouse Balb/3T3 fibroblasts. (A) Flow cytometry histograms of actively dividing and quiescent cells. The percent of cells in each cell cycle phase is shown above the peaks. (B) Amounts of dNTPs in actively dividing and quiescent cells presented as the mean  $\pm$  SEM measured in three independent Balb/3T3 cell extracts. (C) Amounts of NTPs in actively dividing and quiescent cells, presented as the mean  $\pm$  SEM measured in three independent Balb/3T3 cell extracts. (D) Cell volumes of actively dividing and quiescent cells. The horizontal lines indicate the mean  $\pm$  SEM.

**Table 2.** Calibration range, coefficient of determination ( $R^2$ ), lower limit of quantitation (LLOQ), and relative recovery (%) of standard solutions of dNTPs and NTPs

	Calibration range (pmol)	$R^2$	LLOQ (pmol)	Relative recovery (%)
dCTP	0.625, 1.25, 2.5, 5, 10	0.99	0.625	102
dTTP	0.625, 1.25, 2.5, 5, 10	0.99	0.625	92
dATP	0.25, 0.5, 1, 2, 4	0.99	0.25	106
dGTP	0.25, 0.5, 1, 2, 4	0.99	0.25	104
CTP	12.5, 25, 50, 100, 200	0.99	12.5	108
UTP	25, 50, 100, 200, 400	0.99	25	107
ATP	62.5, 125, 250, 500, 1000	0.99	62.5	102
GTP	12.5, 25, 50, 100, 200	0.99	12.5	96

**Table 3.** Intra-day and inter-day precision of measurements of standard solutions of dNTPs and NTPs

Amount (pmol, 5 $\mu$ l injected)	Intra-day precision		Inter-day precision	
	Found $\pm$ SD	%CV	Found $\pm$ SD	%CV
Spiked dCTP				
1	0.86 $\pm$ 0.06	7.3	0.86 $\pm$ 0.01	1.6
2	1.86 $\pm$ 0.09	5.1	1.83 $\pm$ 0.03	1.8
8	7.16 $\pm$ 0.26	3.7	6.88 $\pm$ 0.40	5.8
dTTP				
1	1.20 $\pm$ 0.04	3.0	1.13 $\pm$ 0.05	4.2
2	1.95 $\pm$ 0.03	1.8	1.93 $\pm$ 0.01	0.4
8	8.73 $\pm$ 0.39	4.5	8.15 $\pm$ 0.51	6.3
dATP				
0.4	0.43 $\pm$ 0.01	2.0	0.33 $\pm$ 0.01	3.2
0.8	0.82 $\pm$ 0.06	7.4	0.82 $\pm$ 0.05	5.5
2.5	2.75 $\pm$ 0.10	3.7	2.55 $\pm$ 0.12	4.5
dGTP				
0.4	0.34 $\pm$ 0.04	12.7	0.35 $\pm$ 0.04	10.5
0.8	0.83 $\pm$ 0.04	4.7	0.79 $\pm$ 0.02	2.5
2.5	2.39 $\pm$ 0.15	6.2	2.35 $\pm$ 0.05	2.0
CTP				
20	18.0 $\pm$ 0.6	3.1	18.6 $\pm$ 0.3	1.6
40	36.8 $\pm$ 3.0	8.1	36.6 $\pm$ 2.4	6.6
150	136 $\pm$ 2	1.5	135 $\pm$ 4	2.6
UTP				
40	36.8 $\pm$ 1.1	2.9	38.8 $\pm$ 0.9	2.5
80	76.2 $\pm$ 2.9	3.9	82.1 $\pm$ 8.0	9.8
300	289 $\pm$ 6	2.2	303 $\pm$ 15	5.0
ATP				
100	104 $\pm$ 5	4.7	106 $\pm$ 5	4.5
200	180 $\pm$ 7	3.7	173 $\pm$ 2	1.0
750	684 $\pm$ 34	4.9	654 $\pm$ 28	4.3
GTP				
20	17.0 $\pm$ 0.8	4.6	18.7 $\pm$ 2.4	12.7
40	37.6 $\pm$ 1.6	4.2	34.6 $\pm$ 1.1	3.1
150	154 $\pm$ 6	3.6	152 $\pm$ 1.2	0.8

**Table 4.** Amounts (pmol/ $10^6$  cells) of dNTPs and NTPs in actively dividing (log) and quiescent (24 and 48 h) mouse Balb/3T3 fibroblasts. Quiescence was achieved by serum starvation for 24 or 48 h

	CTP	dCTP	UTP	dTTP	ATP	dATP	GTP	dGTP
Log	1955	70	4095	92	7454	44	1531	18
24 h	1110	15	2300	14	6059	5	1389	3
48 h	960	13	2070	10	5848	5	1417	1.6

**Table 5.** Ratios of NTP/dNTP in actively dividing (log) and quiescent (24 and 48 h) mouse Balb/3T3 fibroblasts. Quiescence was achieved by serum starvation for 24 or 48 h

	CTP/dCTP	UTP/dTTP	ATP/dATP	GTP/dGTP
Log	28	45	169	85
24 h	74	160	1173	483
48 h	75	204	1150	870

**Table 6.** Concentrations ( $\mu\text{M}$ ) of dNTPs and NTPs in actively dividing (log) and quiescent (24 and 48 h) mouse Balb/3T3 fibroblasts. Quiescence was achieved by serum starvation for 24 or 48 h

	CTP	dCTP	UTP	dTTP	ATP	dATP	GTP	dGTP
Log	647	22	1353	29	2463	14	506	5.6
24 h	367	4.7	760	4.5	2002	1.6	459	0.9
48 h	318	4.0	685	3.2	1932	1.6	468	0.5

thermore, this method can be easily adapted for the measurement of non-canonical minor dNTP species such as dUTP, dITP, 8-oxo-dGTP, and other physiologically relevant dNTPs (39,40). It will be interesting to analyze dNTP and NTP concentrations in various cancer cells, especially in those with mechanistically unexplained mutational signatures, because it might well be that some of such cancer cells have defects in nucleotide metabolism causing increased mutation rates.

The amounts of dNTPs and NTPs per one million mouse Balb/3T3 fibroblasts measured in our study were very close to those previously reported by Ferraro *et al.* for human fibroblasts, including both logarithmically growing and quiescent cells (13). The latter study relied on a DNA polymerase-based assay for determination of dNTPs and on an HPLC-UV-based method for the determination of NTPs. Because the *in vitro* biochemical studies of DNA polymerases require information about the molar concentrations of nucleotides, we went on to measure the cell volumes of the logarithmically growing and quiescent mouse Balb/3T3 fibroblasts and calculated their intracellular dNTP and NTP concentrations (Table 6). We hope that these values will be useful for researchers characterizing mammalian DNA polymerases *in vitro*.

## SUPPLEMENTARY DATA

Supplementary Data are available at NAR Online.

## ACKNOWLEDGEMENTS

We acknowledge the Swedish Metabolomics Centre for support with LC-MS/MS analysis and Irene Martinez Carrasco and the Biochemical Imaging Center at Umeå University and the National Microscopy Infrastructure (NMI) (VR-RFI 2016-00968) for providing assistance in microscopy.

## FUNDING

Swedish Research Council [2014-02262 to A.C., 2017-04028 to R.L.]; Swedish Cancer Society [17 0361 to A.C.]; Kempe Foundation (to Z.K. and S.J.). Funding for open access charge: Vetenskapsrådet [2014-02262 to A.C.].  
*Conflict of interest statement.* None declared.

## REFERENCES

- Reichard,P. (1988) Interactions between deoxyribonucleotide and DNA synthesis. *Annu. Rev. Biochem.*, **57**, 349–374.
- Kunz,B.A., Kohalmi,S.E., Kunkel,T.A., Mathews,C.K., McIntosh,E.M. and Reidy,J.A. (1994) International Commission for Protection Against Environmental Mutagens and Carcinogens. Deoxyribonucleoside triphosphate levels: a critical factor in the maintenance of genetic stability. *Mutat. Res.*, **318**, 1–64.
- Watt,D.L., Buckland,R.J., Lujan,S.A., Kunkel,T.A. and Chabes,A. (2016) Genome-wide analysis of the specificity and mechanisms of replication infidelity driven by imbalanced dNTP pools. *Nucleic Acids Res.*, **44**, 1669–1680.
- Kumar,D., Abdulovic,A.L., Viberg,J., Nilsson,A.K., Kunkel,T.A. and Chabes,A. (2011) Mechanisms of mutagenesis *in vivo* due to imbalanced dNTP pools. *Nucleic Acids Res.*, **39**, 1360–1371.
- Chabes,A., Georgieva,B., Domkin,V., Zhao,X., Rothstein,R. and Thelander,L. (2003) Survival of DNA damage in yeast directly depends on increased dNTP levels allowed by relaxed feedback inhibition of ribonucleotide reductase. *Cell*, **112**, 391–401.
- Mathews,C.K. (2015) Deoxyribonucleotide metabolism, mutagenesis and cancer. *Nat. Rev. Cancer*, **15**, 528–539.
- Thelander,L. (2007) Ribonucleotide reductase and mitochondrial DNA synthesis. *Nat. Genet.*, **39**, 703–704.
- Hakansson,P., Hofer,A. and Thelander,L. (2006) Regulation of mammalian ribonucleotide reduction and dNTP pools after DNA damage and in resting cells. *J. Biol. Chem.*, **281**, 7834–7841.
- Nick McElhinny,S.A., Watts,B.E., Kumar,D., Watt,D.L., Lundstrom,E.B., Burgers,P.M., Johansson,E., Chabes,A. and Kunkel,T.A. (2010) Abundant ribonucleotide incorporation into DNA by yeast replicative polymerases. *Proc. Natl. Acad. Sci. U.S.A.*, **107**, 4949–4954.
- Nick McElhinny,S.A., Kumar,D., Clark,A.B., Watt,D.L., Watts,B.E., Lundstrom,E.B., Johansson,E., Chabes,A. and Kunkel,T.A. (2010) Genome instability due to ribonucleotide incorporation into DNA. *Nat. Chem. Biol.*, **6**, 774–781.
- Williams,J.S., Lujan,S.A. and Kunkel,T.A. (2016) Processing ribonucleotides incorporated during eukaryotic DNA replication. *Nat. Rev. Mol. Cell Biol.*, **17**, 350–363.
- Hollenbaugh,J.A. and Kim,B. (2016) HIV-1 reverse transcriptase-based assay to determine cellular dNTP concentrations. *Methods Mol. Biol.*, **1354**, 61–70.
- Ferraro,P., Franzolin,E., Pontarin,G., Reichard,P. and Bianchi,V. (2010) Quantitation of cellular deoxynucleoside triphosphates. *Nucleic Acids Res.*, **38**, e85.
- Wilson,P.M., Labonte,M.J., Russell,J., Louie,S., Ghobrial,A.A. and Ladner,R.D. (2011) A novel fluorescence-based assay for the rapid detection and quantification of cellular deoxyribonucleoside triphosphates. *Nucleic Acids Res.*, **39**, e112.
- Decosterd,L., Cottin,E., Chen,X., Lejeune,F., Mirimanoff,R., Biollaz,J. and Coucke,P. (1999) Simultaneous determination of deoxyribonucleoside in the presence of ribonucleoside triphosphates in human carcinoma cells by high-performance liquid chromatography. *Anal. Biochem.*, **270**, 59–68.
- Harmenberg,J., Karlsson,A.H. and Gilljam,G. (1987) Comparison of sample preparation methods for the high-performance liquid chromatographic analysis of cell culture extracts for triphosphate ribonucleosides and deoxyribonucleosides. *Anal. Biochem.*, **161**, 26–31.
- Cross,D., Miller,B. and James,S. (1993) A simplified HPLC method for simultaneously quantifying ribonucleotides and deoxyribonucleotides in cell extracts or frozen tissues. *Cell Prolifer.*, **26**, 327–336.
- Shewach,D.S. (1992) Quantitation of deoxyribonucleoside 5'-triphosphates by a sequential boronate and anion-exchange high-pressure liquid chromatographic procedure. *Anal. Biochem.*, **206**, 178–182.
- Di Piero,D., Tavazzi,B., Perno,C.F., Bartolini,M., Balestra,E., Calì,R., Giardina,B. and Lazzarino,G. (1995) An ion-pairing high-performance liquid chromatographic method for the direct simultaneous determination of nucleotides, deoxynucleotides, nicotinic coenzymes, oxypurines, nucleosides, and bases in perchloric acid cell extracts. *Anal. Biochem.*, **231**, 407–412.

20. Cohen,S., Megherbi,M., Jordheim,L.P., Lefebvre,I., Perigaud,C., Dumontet,C. and Guittton,J. (2009) Simultaneous analysis of eight nucleoside triphosphates in cell lines by liquid chromatography coupled with tandem mass spectrometry. *J. Chromatogr. B*, **877**, 3831–3840.
21. Henneré,G., Becher,F., Pruvost,A., Goujard,C., Grassi,J. and Benech,H. (2003) Liquid chromatography–tandem mass spectrometry assays for intracellular deoxyribonucleotide triphosphate competitors of nucleoside antiretrovirals. *J. Chromatogr. B*, **789**, 273–281.
22. Alpert,A.J. (1990) Hydrophilic-interaction chromatography for the separation of peptides, nucleic acids and other polar compounds. *J. Chromatogr. A*, **499**, 177–196.
23. Ikegami,T., Tomomatsu,K., Takubo,H., Horie,K. and Tanaka,N. (2008) Separation efficiencies in hydrophilic interaction chromatography. *J. Chromatogr. A*, **1184**, 474–503.
24. Hemstrom,P. and Irgum,K. (2006) Hydrophilic interaction chromatography. *J. Sep. Sci.*, **29**, 1784–1821.
25. McCalley,D.V. (2017) Understanding and manipulating the separation in hydrophilic interaction liquid chromatography. *J. Chromatogr. A*, **1523**, 49–71.
26. Johnsen,E., Wilson,S.R., Odsbu,I., Krapp,A., Malerod,H., Skarstad,K. and Lundanes,E. (2011) Hydrophilic interaction chromatography of nucleoside triphosphates with temperature as a separation parameter. *J. Chromatogr. A*, **1218**, 5981–5986.
27. Olafsson,S., Whittington,D., Murray,J., Regnier,M. and Moussavi-Harami,F. (2017) Fast and sensitive HPLC–MS/MS method for direct quantification of intracellular deoxyribonucleoside triphosphates from tissue and cells. *J. Chromatogr. B Analyt. Technol. Biomed. Life Sci.*, **1068–1069**, 90–97.
28. Qian,T., Cai,Z. and Yang,M.S. (2004) Determination of adenosine nucleotides in cultured cells by ion-pairing liquid chromatography–electrospray ionization mass spectrometry. *Anal. Biochem.*, **325**, 77–84.
29. Dietmair,S., Timmins,N.E., Gray,P.P., Nielsen,L.K. and Krömer,J.O. (2010) Towards quantitative metabolomics of mammalian cells: development of a metabolite extraction protocol. *Anal. Biochem.*, **404**, 155–164.
30. Hofer,A., Ekanem,J.T. and Thelander,L. (1998) Allosteric regulation of *Trypanosoma brucei* ribonucleotide reductase studied in vitro and in vivo. *J. Biol. Chem.*, **273**, 34098–34104.
31. Deem,A., Keszthelyi,A., Blackgrove,T., Vayl,A., Coffey,B., Mathur,R., Chabes,A. and Malkova,A. (2011) Break-induced replication is highly inaccurate. *PLoS Biol.*, **9**, e1000594.
32. Davidson,M.B., Katou,Y., Keszthelyi,A., Sing,T.L., Xia,T., Ou,J., Vaisica,J.A., Thevakumaran,N., Marjavaara,L., Myers,C.L *et al.* (2012) Endogenous DNA replication stress results in expansion of dNTP pools and a mutator phenotype. *EMBO J.*, **31**, 895–907.
33. Poli,J., Tsaponina,O., Crabbe,L., Keszthelyi,A., Pantesco,V., Chabes,A., Lengronne,A. and Pasero,P. (2012) dNTP pools determine fork progression and origin usage under replication stress. *EMBO J.*, **31**, 883–894.
34. Gupta,A., Sharma,S., Reichenbach,P., Marjavaara,L., Nilsson,A.K., Lingner,J., Chabes,A., Rothstein,R. and Chang,M. (2013) Telomere length homeostasis responds to changes in intracellular dNTP pools. *Genetics*, **193**, 1095–1105.
35. Buckland,R.J., Watt,D.L., Chittoor,B., Nilsson,A.K., Kunkel,T.A. and Chabes,A. (2014) Increased and imbalanced dNTP pools symmetrically promote both leading and lagging strand replication infidelity. *PLoS Genet.*, **10**, e1004846.
36. Mertz,T.M., Sharma,S., Chabes,A. and Shcherbakova,P.V. (2015) Colon cancer-associated mutator DNA polymerase delta variant causes expansion of dNTP pools increasing its own infidelity. *Proc Natl. Acad. Sci. U.S.A.*, **112**, E2467–E2476.
37. Williams,L.N., Marjavaara,L., Knowels,G.M., Schultz,E.M., Fox,E.J., Chabes,A. and Herr,A.J. (2015) dNTP pool levels modulate mutator phenotypes of error-prone DNA polymerase epsilon variants. *Proc. Natl. Acad. Sci. U.S.A.*, **112**, E2457–E2466.
38. Kochenova,O.V., Bezalel-Buch,R., Tran,P., Makarova,A.V., Chabes,A., Burgers,P.M. and Shcherbakova,P.V. (2017) Yeast DNA polymerase zeta maintains consistent activity and mutagenicity across a wide range of physiological dNTP concentrations. *Nucleic Acids Res.*, **45**, 1200–1218.
39. Fouquerel,E., Lormand,J., Bose,A., Lee,H.T., Kim,G.S., Li,J., Sobol,R.W., Freudenthal,B.D., Myong,S. and Opreško,P.L. (2016) Oxidative guanine base damage regulates human telomerase activity. *Nat. Struct. Mol. Biol.*, **23**, 1092–1100.
40. Pang,B., McFaline,J.L., Burgis,N.E., Dong,M., Taghizadeh,K., Sullivan,M.R., Elmquist,C.E., Cunningham,R.P. and Dedon,P.C. (2012) Defects in purine nucleotide metabolism lead to substantial incorporation of xanthine and hypoxanthine into DNA and RNA. *Proc. Natl. Acad. Sci. U.S.A.*, **109**, 2319–2324.